The $K_{\ell3}$ Form Factors and
Atmospheric Neutrino Flavor Ratio at High Energies

V. A. Naumov, [1,2,3] T. S. Sinegovskaya, [2] S. I. Sinegovsky, [2]

[1] *Laboratory of Theoretical Physics, Irkutsk State University, Irkutsk 664003, Russia*
[2] *Department of Theoretical Physics, Physics Faculty, Irkutsk State University, Irkutsk 664003, Russia*
[3] *Istituto Nazionale di Fisica Nucleare, Sezione di Firenze, Firenze 50125, Italy*

We calculated the differential and total rates for the semileptonic decays of K_L^0 and $K^\pm$ mesons taking into account a linear q^2 dependence of the $K_{\ell3}$ form factors. As a case in point, we included these rates into the calculation of the atmospheric neutrino flux at energies 1 to 100 TeV. The calculated neutrino spectra are between the earlier predictions while the neutrino flavor ratio, R, is somewhat affected by the $K_{\ell3}$ form factors. The R proves to be very sensitive to the contribution of neutrinos from decay of charmed particles, providing an additional method to test the charm production models in future experiments with large-volume neutrino telescopes.

PACS numbers: 13.20.Eb, 13.85.Tp, 96.40.Tv

I. INTRODUCTION

Atmospheric neutrinos (AN) come from the decays of unstable particles generated in the collisions of primary and secondary cosmic rays with air nuclei. Up to very high energies, the dominant contribution is due to decays of charged pions, charged and long-lived neutral kaons. The AN from these sources have come to be known as "π, K" or conventional neutrinos. As energy increases, semileptonic decays of charmed hadrons (mainly $D^\pm$, D^0, $\overline{D}^0$, $D_s^\pm$ mesons and Λ_c^+ hyperons) should become important. These AN are usually called prompt neutrinos (PN). The borderline energy between the domination regions of conventional and prompt neutrinos is a long-standing question. Taking into account the available data on cosmic-ray muons [1], it is safe to say that the PN fraction in the vertical (horizontal) muon neutrino flux is negligible at energies below $E_\nu^b \sim 1\,TeV$ ($\sim 10\,TeV$); for the electron neutrino flux, the corresponding borders are roughly an order of magnitude less. But it is not excluded that E_ν^b may be increased by 10 to 100 times.

The AN flux with energies above 1 TeV represents an unavoidable background for many of the astrophysical experiments with the full-size underwater/ice neutrino telescopes[1]. At the same time, the AN flux is a natural tool for studying neutrino interactions with matter and, along with the atmospheric muon flux, it provides a way of testing the inputs of nuclear cascade models that is parameters of the primary cosmic-ray flux and cross sections of hadron-nucleus interactions at energies beyond the reach of accelerator experiments. In particular, the AN flux measurements have much potential for yielding information about the mechanism of charm production.

In both cases – to correct for the AN background and to use the AN flux as an additional tool of particle physics – it is necessary to know with confidence the conventional AN flux. The relevant calculations have been performed by many authors (see [2–8] and references therein). The discrepancy between the different predictions for the π, K neutrino flux above 1 TeV ranges up to 25–35 % for $\nu_\mu + \overline{\nu}_\mu$ and to 60–70 % for $\nu_e + \overline{\nu}_e$ (depending upon the zenith angle). Unfortunately, these numbers are not representative of the upper limits for the calculation uncertainty. For the most part this is due to the incompleteness in the current knowledge of the primary spectrum and composition as well as mechanisms of π and, to a greater extent, K meson production at high energies (see [6] for a detailed discussion). A sizable part of the discrepancy is caused by different approximations and simplifications employed in the calculations.

Predictions for the PN contribution vary by a few orders of magnitude (see [7–9] and references therein). Here, the basic challenge is of course in the mechanism of charm hadroproduction. An additional (though not so drastic) source of uncertainty has to do with the differential rates of inclusive semileptonic decays of charmed hadrons. The theory of charm production and decay is still far from completion and the corresponding accelerator data are rather meagre. However, when correlating the predictions of different models with each other and with experiment, the neglecting some comparatively small effects may introduce additional systematic errors and should be avoided.

---

[1] Among them the detection of neutrinos from the (quasi)diffuse neutrino backgrounds, like pregalactic neutrinos, neutrinos from the bright phase of galaxy evolution and from active galactic nuclei.

Some relative characteristics of the AN flux, like the zenith-angle distribution and the flavor ratio,

$$R = \frac{\nu_\mu + \overline{\nu}_\mu}{\nu_e + \overline{\nu}_e},$$

prove to be less sensitive to the uncertainties of the conventional AN flux predictions and, on the other hand, they are very dependent of the PN contribution. The latter is owing to the salient and model-independent features of the PN flux. First, it is almost isotropic within a wide energy range[2] and second, the $\nu/\overline{\nu}$ ratio and the flavour ratio, R, are both about 1. These features provide a way to discriminate the PN contribution through the analysis of the angular distribution and the relationship between the muon and electron neutrino-induced events in a neutrino telescope.

In this paper we calculate the conventional AN energy spectra with taking into account one additional effect which was ignored in all previous AN flux calculations, – the dependence of the $K_{\ell 3}^\pm$ and $K_{\ell 3}^0$ decay form factors on q^2 (where q is the 4-momentum transfer to the lepton pair). Inclusion of the q^2-dependent form factors causes certain changes in the differential $K_{\ell 3}$ decay rates and therefore it should affect the overall π, K neutrino flux. Magnitude of the effect is wittingly small, but it is energy-dependent and opposite in sign for muon and electron neutrinos; consequently it must change predictions for the R as a function of energy. The $K_{\ell 3}$ decay contribution is "by definition" negligible at energies where the prompt neutrinos become important. But, let us recall, the borderline energy remains unknown for the present and hence the effect under consideration might be interesting up to the PeV energy range.

In the next Section we present some necessary formulas from the theory of neutrino production in the atmosphere. Section III deals with the differential and total $K_{\ell 3}$ decay rates. In Section IV we briefly describe our nuclear cascade model. Section V is devoted to the discussion of our results for the AN spectra, while the conclusions are in Section VI.

II. NEUTRINO PRODUCTION IN THE ATMOSPHERE

Let P labels a particle which can produce a lepton pair $\overline{\ell}\nu_\ell$ or $\ell\overline{\nu}_\ell$ ($\ell = e, \mu$) on decay and $\Phi_P(E_P, z, \vartheta)$ be the differential energy spectrum of these particles as a function of energy E_P, atmospheric depth z and zenith angle ϑ. Let $d\Gamma_{P_{\ell k}}^\nu/dE_\nu$ be the differential with respect to neutrino energy E_ν rate for the k-body decay mode $P_{\ell k}$, as a function of E_P and E_ν in the laboratory frame of reference (the symbol ν stands for ν_ℓ or $\overline{\nu}_\ell$). Then the differential energy spectrum of neutrinos at the depth z and zenith angle ϑ is given by

$$\Phi_\nu(E_\nu, z, \vartheta) = \sum_P \sum_k \int_0^z \int_{E_{P_{\ell k}}}^\infty \left[\frac{d\Gamma_{P_{\ell k}}^\nu(E_P, E_\nu)}{dE_\nu} \right] \Phi_P(E_P, z', \vartheta) \frac{dz' dE_P}{\rho(z', \vartheta)}, \qquad (2.1)$$

where $\rho(z, \vartheta)$ is the air density on the corresponding altitude in the atmosphere in terms of variables z and ϑ; the summation is over all particles P and k-body decay modes.

The main decay modes answerable for the conventional neutrino production are $\mu_{e3}^\pm$, $\pi_{\mu 2}^\pm$, $K_{\mu 2}^\pm$, $K_{\ell 3}^\pm$ and $K_{\ell 3}^0$. Prompt neutrinos are produced through the multiple modes of semileptonic decays of charmed hadrons but, considering sizable gaps in the experimental data [10] and certain difficulties in the theoretical description of charm decay, it is instructive (and generally accepted) to use the inclusive approach.

The lower limit of integration over E_P in eq. (2.1) is defined by kinematics ($c = 1$). At $E_\nu \gg 1\ GeV$,

$$E_{P_{\ell k}} = \left(m_P^2 / M_{P_{\ell k}}^2 \right) E_\nu,$$

where

$$M_{\mu e3}^2 = m_\mu^2, \quad M_{\pi_{\mu 2}}^2 = m_\pi^2 - m_\mu^2,$$

$$M_{K_{\mu 2}}^2 = m_K^2 - m_\mu^2, \quad M_{K_{\ell 3}}^2 = m_K^2 - m_\pi^2 + m_\ell^2,$$

and, for the inclusive decays,

$$M_{P \to \overline{\ell}\nu X}^2 = m_P^2 + m_\ell^2 - s_X^{\min}$$

---

[2]Namely, at $10\ TeV < E_\nu < 3 \cdot 10^3\ TeV$, the maximum anisotropy is about 3–4 % [7].

with $s_X^{\min}$ the invariant mass square minimum.

The total rate of the $P_{\ell k}$ decay in the lab. frame is defined by

$$\Gamma(P_{\ell k}) = \int \left[\frac{d\Gamma^\nu_{P_{\ell k}}(E_P, E_\nu)}{dE_\nu} \right] dE_\nu = \frac{B(P_{\ell k}) m_P}{\tau_P E_P},$$

where m_P and τ_P are the mass and life time of the particle P, respectively, and $B(P_{\ell k})$ is the $P_{\ell k}$ decay branching ratio. Let us introduce the "spectral function"

$$F^\nu_{P_{\ell k}} = \frac{E_P}{\Gamma(P_{\ell k})} \left[\frac{d\Gamma^\nu_{P_{\ell k}}(E_P, E_\nu)}{dE_\nu} \right].$$

It can be shown that, in the ultrarelativistic limit, the $F^\nu_{P_{\ell k}}$ is a function of the only dimensionless variable $x = E_\nu/E_P$ $(0 < x < M^2_{P_{\ell k}}/m^2_P)$.

The spectral function for any two-body decay is merely constant. In particular,

$$F^{\nu_\mu(\overline{\nu}_\mu)}_{\pi_{\mu 2}} = \frac{1}{1 - m^2_\mu/m^2_\pi}, \qquad F^{\nu_\mu(\overline{\nu}_\mu)}_{K_{\mu 2}} = \frac{1}{1 - m^2_\mu/m^2_K}.$$

The spectral functions for the three-particle decay of a polarized muon in the ultrarelativistic limit are of the form [12]

$$F^{\nu_e(\overline{\nu}_e)}_{\mu_{e3}}(x) = 2(1-x)^2 \left[1 + 2x \pm \mathcal{P}_\mu(1 - 4x) \right],$$

$$F^{\nu_\mu(\overline{\nu}_\mu)}_{\mu_{e3}}(x) = \frac{1}{3}(1-x) \left[5 + 5x - 4x^2 \pm \mathcal{P}_\mu(1 + x - 8x^2) \right],$$

where $\mathcal{P}_\mu$ is the muon polarization dependent on the muon and parent meson momenta. These dependencies are different for the different meson decay modes. The μ-decay contribution into the $\nu_\mu + \overline{\nu}_\mu$ flux is very small at high energies but in contrast, it dominates in the $\nu_e + \overline{\nu}_e$ flux up to about 100 GeV for vertical and to several hundreds of GeVs for horizontal directions. The muon polarization is therefore an essential factor affecting the neutrino flavor ratio and the neutrino to antineutrino ratio [5,11]. However, at $E_\nu > 1\,TeV$ one can greatly simplify matter treating the $\mathcal{P}_\mu$ as an effective constant, $\langle \mathcal{P}_\mu \rangle$. In our calculations we adopt $\langle \mathcal{P}_\mu \rangle = 0.33$. Besides, as is customary in all AN flux calculations, we take no account of a small change of the shape of neutrino distributions which result from the radiative mode $\mu \to e\overline{\nu}_e\nu_\mu\gamma$ (with branching ratio of $(1.4 \pm 0.4)\,\%$) but simply increase the $B(\mu_{e3})$ to $100\,\%$.

The spectral functions for the three-particle kaon decays calculated without considering the $K_{\ell 3}$ form factors can be found in [2] and [5]. The inclusion of the q^2-dependent form factors is the subject of the next Section. One more point need to be made here. As in the case with μ-decay, below we neglect the radiative mode $K^0_L \to \pi e\overline{\nu}_e\gamma$ (branching ratio is $(1.3 \pm 0.8)\,\%$) but increase the $B(K^0_{e3})$ to $40\,\%$ (cf. [10]). This approximation yields a completely negligible change in the $\nu_e + \overline{\nu}_e$ flux.

In this paper, we will not enlarge on the calculation of the spectral functions for the inclusive semileptonic decays of charmed hadrons. Our simple phenomenological approach to the problem has been described in [7].

III. $K_{\ell 3}$ DECAYS

In the standard theory of weak interactions, the $K_{\ell 3}$ decay matrix element can be written in the form

$$\frac{G_F}{\sqrt{2}} \sin\theta_C \left[f_+(q^2)(p_K + p_\pi)^\mu + f_-(q^2)(p_K - p_\pi)^\mu \right] \overline{\ell}\gamma_\mu(1 + \gamma_5)\nu_\ell. \tag{3.1}$$

Here G_F and θ_C are the Fermi constant and Cabibbo angle, $p_{K,\pi}$ are the 4-momenta of the kaon and pion, and $f_\pm(q^2)$ are dimensionless form factors which are real functions of $q^2 = (p_K - p_\pi)^2$, the square of the 4-momentum carried by leptons. Experimental investigations of $K_{\ell 3}$ decays suggest that the form factors $f_\pm(q^2)$ are smooth functions of q^2 which are normally written in the linear approximation as

$$f_\pm(q^2) = f_\pm(0) \left(1 + \lambda_\pm \frac{q^2}{m^2_\pi} \right). \tag{3.2}$$

In the limit of unbroken $SU(3)$ symmetry,

$$f_+(0) = 1 \quad \text{for} \quad K^0_{\ell 3} \quad \text{and} \quad f_+(0) = \frac{1}{\sqrt{2}} \quad \text{for} \quad K^\pm_{\ell 3}, \tag{3.3}$$

3

while $f_-(0)$ reduces to zero. As a consequence, the parameter $\xi = f_-(0)/f_+(0)$ should be small for K_{e3} decays (the Ademollo-Gatto theorem) [13]. In the $K_{\mu3}$ case, the Ademollo-Gatto theorem is not valid and so, it is not forbidden that $\xi \sim 1$. The absolute normalization of the $K_{\ell3}$ decay rates is not warranted for our purposes, as we use the experimental values for $B(K_{\ell3})$ and τ_K. This being so, we adopt eqs. (3.2,3.3) from here on, considering $\lambda_\pm$ and ξ as input parameters.

From eqs. (3.1) and (3.2), using standard techniques [14], we find the differential (with respect to neutrino energy) and total $K_{\ell3}$ decay rates in the lab. frame of reference. In a general way, the $K_{\ell3}$ spectral function may be written as [15]

$$F^\nu_{K_{\ell3}}(x) = \frac{1}{Z} \sum_{n=-4}^{3} C_n J_n(x),$$

with the normalization constant

$$Z = \sum_{n=-4}^{3} C_n \left[J_{n+1}(0) - J_n(0) \right].$$

Here

$$J_n(x) = \int_{y_+}^{1-x} dy\, y^n \sqrt{(y - y_+)(y - y_-)}, \qquad y_\pm = \frac{(m_\pi \pm m_\ell)^2}{m_K^2},$$

(these integrals are expressible in terms of elementary functions) and C_n are the constants proportional to $f_+^2(0)$ and dependent on the masses, m_K, m_π, m_ℓ and the parameters $\lambda_\pm$ and ξ. Let us define $C_n = f_+^2(0)c_n$. Then the coefficients c_n are

$$c_{-4} = -6r_\ell(r - r_\ell)^3 v^2 \lambda^2,$$

$$\begin{aligned} c_{-3} =\ & 8r_\ell(r - r_\ell)^2 uv\lambda - 2(r - r_\ell)\{4(r - r_\ell)[r - r_\ell(1 - 4v)] \\ & -r_\ell[3r(1 + 3r) - r_\ell(9 + 10r - r_\ell)]v^2\}\lambda^2, \end{aligned}$$

$$\begin{aligned} c_{-2} =\ & -3r_\ell(r - r_\ell)u^2 + 4\{2(r - r_\ell)[2(r - r_\ell) + 3r_\ell(u + v)] \\ & -r_\ell[r + r_\ell + (r - r_\ell)(3 + 4r - r_\ell)]uv\}\lambda \\ & +8\{(r - r_\ell)[(r - r_\ell)(4 + 3r + r_\ell) - (r + r_\ell)] + 4r_\ell[r(2 + 3r) - r_\ell(1 + 3r)]v\}\lambda^2 \\ & -2r_\ell\{(r - r_\ell)[3(2 + 8r + 3r^2) - r_\ell(2r + r_\ell)] + (r + r_\ell)(3 + 3r + r_\ell)\}v^2\lambda^2, \end{aligned}$$

$$\begin{aligned} c_{-1} =\ & -3\{4r - r_\ell[4(1 - 2u) + (1 + r - r_\ell)u^2]\} - 4\{8r(1 + r) - 4r_\ell(4 + r + r_\ell) \\ & +r_\ell[2(1 + 4r + r^2) - r_\ell(1 + r + r_\ell)]uv - 6r_\ell(1 + 2r)(u + v)\}\lambda \\ & -8\{3r(1 + 3r + r^2) - r_\ell[5 + 16r + r^2 + r_\ell(1 + r + r_\ell) \\ & +2(5 + 15r + 6r^2 + 3r_\ell)v]\lambda^2 + 2r_\ell\{3(1 + r)(1 + 9r + r^2) \\ & +r_\ell[3 + 4r + r^2 + r_\ell(4 + r + r_\ell)]\}v^2\lambda^2, \end{aligned}$$

$$\begin{aligned} c_0 =\ & 3\{4(1 + r) - r_\ell[4 + (u - 8)u]\} + 4\{4(1 + 4r + r^2) \\ & -r_\ell[4(5 - r + 2r_\ell) - 6(2 + r + r_\ell)(u + v) + (4 + 4r + r_\ell)uv]\}\lambda \\ & +8\{(1 + r)(1 + 8r + r^2 - r_\ell[3 - 4r - r^2 + r_\ell(3 - r + 3r_\ell)]\}\lambda^2 \\ & +2r_\ell\{16[3 + 6r + r^2 + r_\ell(3 + r + r_\ell)] - [9(1 + 3r + r^2) + r_\ell(7 + 4r + r_\ell)]v\}v\lambda^2, \end{aligned}$$

$$\begin{aligned} c_1 =\ & -12 - 8\{4(1 + r) - r_\ell[2 - 3(u + v) - uv]\}\lambda - 2\{12(1 + 3r + r^2) \\ & -r_\ell[4(7 + 5r_\ell) - 32(3 + 2r + 2r_\ell)v + (9 + 9r + 5r_\ell)v^2]\}\lambda^2, \end{aligned}$$

$$c_2 = 16\lambda + 2\{12(1 + r) - r_\ell[4 - (16 - 3v)v]\}\lambda^2,$$

$$c_3 = -8\lambda^2,$$

4

where we used the following notation:

$$r = \frac{m_\pi^2}{m_K^2}, \qquad r_\ell = \frac{m_\ell^2}{m_K^2},$$

and

$$u = 1 - \xi, \qquad v = 1 - \xi \frac{\lambda_-}{\lambda_+}, \qquad \lambda = \frac{\lambda_+}{2r}.$$

To estimate the numerical values for the C_n, we use the parameters λ_+ and ξ evaluated by the Particle Data Group [10] (see table I).

TABLE I. $K_{\ell3}$ form factor parameters [10].

	K_{e3}^0	$K_{\mu3}^0$	$K_{e3}^\pm$	$K_{\mu3}^\pm$
λ_+	0.0300 ± 0.0016	0.034 ± 0.005	0.0286 ± 0.0022	0.033 ± 0.008
ξ		-0.11 ± 0.09		-0.35 ± 0.15

Since the term of the matrix element (3.1) proportional to f_- can be neglected for K_{e3} and most $K_{\mu3}$ data are adequately described with a constant f_- [10], in the subsequent discussion we assume $\lambda_- = 0$. The numerical values of the coefficients C_n are given in tables II and III. For comparison we also included in these tables the C_n calculated with $\lambda_+ = 0$.

In the K_{e3} case, electron mass can be neglected as compared to pion mass. In this approximation, one can easily found

$$F_{K_{e3}}^{\nu_e}(x) = \frac{1}{Z} \left\{ \frac{rC_{-3}}{2(1-x)^2} + \frac{rC_{-2} - C_{-3}}{1-x} + (C_{-2} - rC_{-1})\ln(1-x) + C_{-1}(1-x) \right.$$
$$+ \sum_{n=0}^{3} C_n \left[(1-x)^{n+1} \left(\frac{1-x}{n+2} - \frac{r}{n+1} \right) + \frac{r^{n+2}}{(n+1)(n+2)} \right]$$
$$\left. + \frac{C_{-3}}{2r} - C_{-2}(\ln r + 1) + rC_{-1}(\ln r - 1) \right\}, \tag{3.4}$$

where

$$Z = [(1+r)C_{-2} - C_{-3} - rC_{-1}]\ln r + 2(1-r)C_{-2} - \frac{1-r^2}{2r}(C_{-3} + rC_{-1})$$
$$+ \sum_{n=0}^{3} C_n \left[\frac{r(1-r^{n+1})}{(n+1)(n+2)} - \frac{1-r^{n+3}}{(n+2)(n+3)} \right] \tag{3.5}$$

and $r = m_\pi^2/m_K^2$. The total K_{e3} decay rate in the rest frame has the form (cf. [13])

$$\Gamma^*(K_{e3}) = \frac{G_F^2 \sin^2 \theta_C m_K^5}{768\pi^3} f_+^2(0) \left(a_0 + a_1\lambda_+ + a_2\lambda_+^2 \right), \tag{3.6}$$

with constant a_i. Substituting the numerical values of the parameters yields

$$a_0 \simeq 0.576, \quad a_1 \simeq 2.140, \quad a_2 \simeq 1.580 \quad \text{for} \quad K_{e3}^\pm,$$
$$a_0 \simeq 0.560, \quad a_1 \simeq 1.947, \quad a_2 \simeq 1.345 \quad \text{for} \quad K_{e3}^0.$$

Let us pass over the explicit form of the $F_{K_{\mu3}}^{\nu_\mu}(x)$ and $\Gamma^*(K_{\mu3})$ which is much more complicated in comparison with eqs. (3.4–3.6), and proceed to some numerical results. Figures 1 and 2 show respectively the $K_{\ell3}$ spectral functions and differential decay rates (versus x) calculated with $f_+ = f_+(0)$ and with the q^2-dependent form factors. As is seen from fig. 1, the effect for the spectral functions is different in magnitude and, more importantly, opposite for electron and muon neutrinos, even though the absolute differential rates (fig. 2) grow if the form factors are accounted for. As a result, the $K_{\ell3}$ contribution to the AN flux shall slightly be increased for electron neutrinos and decreased for muon neutrinos, compared to the case of constant form factors. Clearly, in the range where the conventional neutrinos

TABLE II. Coefficients C_n for $K_{\ell 3}^0$ decays ($\lambda_- = 0$, $\xi = -0.11$).

C_n	$K_L^0 \to \pi^\pm e^\mp \overline{\nu}_e\,(\nu_e)$		$K_L^0 \to \pi^\pm \mu^\mp \overline{\nu}_\mu\,(\nu_\mu)$	
	$\lambda_+ = 0$	$\lambda_+ = 0.030$	$\lambda_+ = 0$	$\lambda_+ = 0.034$
C_{-4}	0	0	0	$-1.99 \cdot 10^{-8}$
C_{-3}	0	$-5.90 \cdot 10^{-6}$	0	$3.78 \cdot 10^{-6}$
C_{-2}	0	$1.03 \cdot 10^{-3}$	$-2.29 \cdot 10^{-4}$	$4.33 \cdot 10^{-4}$
C_{-1}	$-3.93 \cdot 10^{-2}$	$-6.45 \cdot 10^{-2}$	$-5.93 \cdot 10^{-2}$	$-7.94 \cdot 10^{-2}$
C_0	$5.39 \cdot 10^{-1}$	$7.29 \cdot 10^{-1}$	$5.60 \cdot 10^{-1}$	$7.80 \cdot 10^{-1}$
C_1	$-5.00 \cdot 10^{-1}$	$-8.19 \cdot 10^{-1}$	$-5.00 \cdot 10^{-1}$	$-8.82 \cdot 10^{-1}$
C_2	0	$1.66 \cdot 10^{-1}$	0	$1.96 \cdot 10^{-1}$
C_3	0	$-1.21 \cdot 10^{-2}$	0	$-1.56 \cdot 10^{-2}$

TABLE III. Coefficients C_n for $K_{\ell 3}^\pm$ decays ($\lambda_- = 0$, $\xi = -0.35$).

C_n	$K^\pm \to \pi^0 e^\pm \nu_e\,(\overline{\nu}_e)$		$K^\pm \to \pi^0 \mu^\pm \nu_\mu\,(\overline{\nu}_\mu)$	
	$\lambda_+ = 0$	$\lambda_+ = 0.0286$	$\lambda_+ = 0$	$\lambda_+ = 0.0330$
C_{-4}	0	0	0	$-6.77 \cdot 10^{-9}$
C_{-3}	0	$-2.55 \cdot 10^{-6}$	0	$1.95 \cdot 10^{-6}$
C_{-2}	0	$4.66 \cdot 10^{-4}$	$-1.51 \cdot 10^{-4}$	$1.17 \cdot 10^{-4}$
C_{-1}	$-1.87 \cdot 10^{-2}$	$-3.06 \cdot 10^{-2}$	$-3.28 \cdot 10^{-2}$	$-4.31 \cdot 10^{-2}$
C_0	$2.69 \cdot 10^{-1}$	$3.62 \cdot 10^{-1}$	$2.83 \cdot 10^{-1}$	$3.96 \cdot 10^{-1}$
C_1	$-2.50 \cdot 10^{-1}$	$-4.10 \cdot 10^{-1}$	$-2.50 \cdot 10^{-1}$	$-4.46 \cdot 10^{-1}$
C_2	0	$8.34 \cdot 10^{-2}$	0	$1.01 \cdot 10^{-1}$
C_3	0	$-6.10 \cdot 10^{-3}$	0	$-8.12 \cdot 10^{-3}$

TABLE IV. $K_{\ell 3}$ decay rates.

Decay mode	Calculated with $f_+ = f_+(0)$ (10^6 s^{-1})	Calculated with $f_+ = f_+(q^2)$ (10^6 s^{-1})	Experimental best fit [10] (10^6 s^{-1})
K_{e3}^0	6.76	7.49	7.49 ± 0.06
$K_{\mu 3}^0$	4.38	5.25	5.25 ± 0.05
$K_{e3}^\pm$	3.34	3.70	3.89 ± 0.05
$K_{\mu 3}^\pm$	2.06	2.50	2.57 ± 0.06

dominate, the magnitude of the effect in the overall AN flux is determined by the kaon production cross sections that is by the "K/π ratio" and, to a lesser extend, by the cross sections for kaon regeneration.

In table IV we give the decay rates, $\Gamma^*(K_{\ell 3})$, calculated using the above formulas with $f_+ = f_+(0)$ and with the linear dependence of f_+ on q^2 (3.2), together with the best fits of experimental data obtained by the Particle Data Group [10].

As table IV suggests, the inclusion of the q^2-dependent form factors causes the increase of about 11 % in the K_{e3} decay rates and of about 20 % in the $K_{\mu 3}$ rates. The improved rates correlate well with the experimental data except the $K_{e3}^\pm$ case. But the latter is not an essential flaw, having regard to the variance of the world data on $\Gamma^*(K_{e3}^\pm)$ which is far more than the error of the PDG best fit. The additional corrections due to the $SU(3)$ symmetry breaking should be less than 3–4 % and, what is more essential for our study, they cannot change the spectral functions, $F_{K_{\ell 3}}^\nu(x)$, that is the shape of the neutrino distributions from $K_{\ell 3}$ decays.

IV. NUCLEAR CASCADE MODEL

Our nuclear cascade calculations are based on the model by Vall et al. [16]. The results obtained within this model agree well with all available experimental data on hadron spectra (including the single proton, neutron and pion fluxes) for various atmospheric depths at energies from 1 TeV up to about 600 TeV. The muon spectrum calculated with this model is in reasonable agreement with the current sea-level and underground data [1]. It is also in very good agreement (within 5 %) with the recent Monte Carlo calculation by Agrawal et al. [6].

The model takes into account the processes of regeneration and recharging of nucleons and pions as well as production of kaons, nucleons and charmed hadrons ($D^\pm$, D^0, $\overline{D}^0$, Λ_c^+) in pion–nucleus collisions, muon energy loss, etc. Let

us briefly enumerate here the basic assumptions and discuss some pluses and minuses of the model. Further details and numerical values of the input parameters can be found in [16] for π and K meson production and in [7] for charm production.

(i) Our (analytical) model of the all-particle primary spectra and chemical composition is taken from Nikolsky et al. [17]. This model adequately describes the world data on primary cosmic rays from about 1 TeV/nucleon up to the range well beyond the "knee" region (see a discussion in Bugaev et al. [1]). The nuclear component of the primary flux is treated on the basis of the superposition model.

(ii) We assume a logarithmic growth with energy of the total inelastic cross sections σ_{hA}^{inel} for interactions of a hadron h with a nuclear target A. Such dependence arises from a model for elastic amplitude of hadron–hadron collisions, based on the conception of double pomeron with supercritical intercept. For simplicity sake we also use another consequence of this model, the asymptotic equality of the inelastic cross sections for any projectile hadron. Namely, we assume

$$\sigma_{hA}^{inel}(E_h) = \sigma_{hA} + \sigma_A \ln(E_h/E_1), \qquad \text{for} \quad h = N, \pi, K, D, \Lambda_c,$$

(A is the "air nucleus") at $E_h > E_1 = 1\ TeV$. The calculated cross sections for $h = N, \pi, K$ are in reasonable agreement with available accelerator and cosmic ray data. There are no the data on the inelastic cross sections for charmed hadrons but we notice that the prompt lepton flux is scarcely affected by the specific values of these cross sections up to about $10^4\ TeV$ of lepton energy (due to very short lifetime of charmed particles). Thus even a rough estimation of σ_{DA}^{inel} and $\sigma_{\Lambda_c A}^{inel}$ will suffice for our purposes.

(iii) We assume Feynman scaling in the fragmentation range for the inclusive processes $h_i A \to h_f X$, with $h_i = p, n, \pi^\pm$ and $h_f = p, n, \pi^\pm, K^\pm, K^0, \overline{K}^0$. Thus the invariant inclusive cross sections $E d^3 \sigma_{fi}^A / d^3 p$ are energy independent at large Feynman x. The truth of this assumption is an outstanding question.

(iv) The kaon regeneration (i.e. the processes $K^\pm A \to K^\pm X$, $K^\pm A \to K^0 X$, and so on) is disregarded in our calculations. We also neglect nucleon, pion and charm production in kaon–nucleus collisions as well as pion production in kaon decays, which makes it possible to study the "πN" cascade without reference to kaons. All these simplifications yield a somewhat conservative result for the conventional AN spectra and must be avoided in the future study; the proper inclusion of the kaon regeneration is the most essential point.

(v) At the stage of nuclear cascade (but of course not at the lepton production stage) the decay of charged pions is neglected. This approximation greatly simplifies the description of the pion regeneration/overcharging and nucleon production in pion–nucleus collisions and it is valid at the pion energies above 1–2 TeV for directions close to vertical. However it becomes too crude for near-horizontal directions at $E_\nu < 7 - 8\ TeV$. To extend our results up to 1 TeV, we included the appropriate corrections for pion decay using a numerical procedure.

V. AN FLUX (NUMERICAL RESULTS)

Let us discuss the numerical results presented in figures 3–8.

Figures 3 and 4 show the individual contributions from $\pi_{\mu2}$, $K_{\mu2}^\pm$, $K_{\ell3}^0$, $K_{\ell3}^\pm$ and $\mu_{e3}^\pm$ decays into the $\nu_e + \overline{\nu}_e$ and $\nu_\mu + \overline{\nu}_\mu$ fluxes for vertical and horizontal directions, as well as the overall π, K-neutrino fluxes. As an example of possible PN contribution, we also show the results obtained with the three alternative models for charm hadroproduction: the recombination quark-parton model (RQPM), quark-gluon string model (QGSM) and the model based on perturbative quantum chromodynamics (pQCD). The basic assumptions of the first two models were described by Bugaev et al. [7] (see also [1] and references therein). The third, "state-of-the-art" model was proposed recently by Thunman et al. [8] to simulate charm hadroproduction through pQCD processes. To leading order in the coupling constant, α_s, these are the gluon-gluon fusion and the quark-antiquark annihilation. The next-to-leading order contributions are taken into account by doubling the cross sections. To simulate the primary and cascade interactions, the authors use the well-accepted Monte Carlo code *PYTHYA*.

It is our opinion that the RQPM and QGSM give the safe upper and lower limits for the prompt muon and neutrino fluxes. These limits are not inconsistent with the current deep underground measurements of the muon intensity. However, considering rather strong discrepancy between the data of the ground-based and underground muon experiments [1], the comparatively low prompt muon contribution predicted by the pQCD model cannot be excluded. Similar, very low prompt muon contribution has been evaluated recently by Battistoni et al. [9] using the *DPMJET-II* code based on the two-component dual parton model and interfaced to the shower code *HEMAS*. The calculation of Battistoni et al. [9] does not yield the absolute prompt muon flux but, from the estimated prompt-to-conventional muon ratio, one can see a leastwise qualitative agreement with the result of the pQCD model by Thunman et al. [8]. In particular, both models predict that the prompt muon contribution overcomes the vertical π, K-muon flux in the region of a thousand TeV and therefore is undistinguished in the present-day muon experiments.

As may be seen from fig. 3, the K_{e3} decays give the main contribution into the conventional $\nu_e + \overline{\nu}_e$ flux above 1 TeV independent of zenith angle. The $K_{e3}^{\pm}$ and K_{e3}^0 contributions are practically equal at $\vartheta = 0°$ and close in magnitude at $\vartheta = 90°$, despite the 8-fold difference between the $K_{e3}^{\pm}$ and K_{e3}^0 decay branching ratios. The first reason is that the life time of K_L^0 is about 4.2 times that of $K^{\pm}$. The second one lies in the different inclusive cross sections for $K^+ + K^-$ and $K^0 + \overline{K}^0$ production (see Vall et al. [16]). For the conventional $\nu_\mu + \overline{\nu}_\mu$ flux, the main contribution comes from $K_{\mu2}^{\pm}$ decays (fig. 4). At $\vartheta = 90°$ it stands out above the PN contribution predicted by RQPM, up to about 200 TeV. Second in importance is the $\pi_{\mu2}$ decay contribution. The cross sections for pion production are almost order of magnitude larger than for kaon production, but pion decays become rare above 1 TeV owing to the large life time and Lorentz factor compared to kaon ones. The $K_{\mu3}$ decays give comparatively small contribution which however cannot be neglected. Muon decay contribution is negligible at $\vartheta = 0°$ and very small at $\vartheta = 90°$.

In figures 5 (a–d) we present the conventional $\nu_e + \overline{\nu}_e$ and $\nu_\mu + \overline{\nu}_\mu$ fluxes at $\vartheta = 0°$ and $90°$ as calculated by Volkova [2], Mitsui et al. [3], Butkevich et al. [4], Lipari [5] and Agrawal et al. [6]. All these fluxes are normalized to our one. In the multi-TeV energy range and above, our results fall within the lowest and highest predictions. At $E_\nu < 2 - 3\ TeV$ and $E_\nu < 10\ TeV$ for, respectively, $\vartheta = 0°$ and $\vartheta = 90°$, our calculations give somewhat excessive $\nu_\mu + \overline{\nu}_\mu$ fluxes. In part, this is due to our simplified consideration of the pion decay effect (see Section IV). The corresponding discrepancy is almost negligible for electron neutrinos, since pions give no direct contribution to the $\nu_e + \overline{\nu}_e$ production.

In fig. 6 (a–d) we show our result for the conventional neutrino to antineutrino ratios at $\vartheta = 0°$ and $90°$ (vs. neutrino energy) together with the results of Butkevich et al. [4] and Lipari [5]. The $\nu_e/\overline{\nu}_e$ and $\nu_\mu/\overline{\nu}_\mu$ ratios are very sensitive to the input parameters like the n/p ratio, which is governed by the primary chemical composition, and the π^+/π^-, K^+/K^-, $K^{\pm}/K^0$ ratios, which are determined by the cross sections for the meson production, regeneration and overcharging. Whilst the parameters adopted by Butkevich et al. [4], Lipari [5] and in the present calculation are all within the limits dictated by the available cosmic-ray and accelerator data, the sets of the parameters differ considerably from each other. Consequently, it is no great surprise that the predictions of different models vary over a wide range.

On the other hand, owing to the well-known difference between the cross sections for $\nu_\ell N$ and $\overline{\nu}_\ell N$ charged and neutral current induced interactions, the $\nu_e/\overline{\nu}_e$ and $\nu_\mu/\overline{\nu}_\mu$ ratios are very important inputs for the correct evaluating the neutrino-induced throughgoing muon flux and contained event rate in the neutrino detectors[3]. As is seen from fig. 6, the present-day uncertainty in the $\nu_\mu/\overline{\nu}_\mu$ ratio is not satisfactory. The situation with the $\nu_e/\overline{\nu}_e$ ratio proves to be somewhat better.

Figures 7 (a,b) show the neutrino flavor ratio, R, vs energy at $\vartheta = 0°$ and $90°$. The dashed curves represent the ratio for the conventional AN flux which is a monotonically increasing function of energy varying from about 27.6 to 34.3 at $\vartheta = 0°$ and from about 13.3 to 33.6 at $\vartheta = 90°$ within the interval $1 \div 100\ TeV$. The solid curves are for the R evaluated with taking into account the PN contribution according to three abovementioned models for charm production. The PN contribution results in a decrease of the AN flavor ratio, because the semileptonic decay modes of charmed hadrons with ν_μ ($\overline{\nu}_\mu$) and ν_e ($\overline{\nu}_e$) in the final state have almost the same branching ratios.

As one can see, the R is very sensitive to the charm production model even at energies where the PN contribution remains small in comparison with the conventional one. This effect provides an interesting potential possibility for the experimental discrimination of the PN production by measuring the ratio of the "muonfull" (ν_μ and $\overline{\nu}_\mu$ induced) to "muonless" (ν_e and $\overline{\nu}_e$ induced) contained event rates in a neutrino telescope for different energy thresholds and directions. To a certain extent, such an experiment is easier than the measurement of the absolute neutrino event rate.

Let us briefly sketch now the $K_{\ell3}$ form factor effect. Our calculations show that the effect under discussion is almost independent of zenith angle but quite different for muon and electron neutrinos. At $E_\nu > 1\ TeV$, the effect is identical for the K_{e3}^0 and $K_{e3}^{\pm}$ contributions as well as for the overall $\nu_e + \overline{\nu}_e$ flux (since the K_{e3} decays are the main source of ν_e and $\overline{\nu}_e$); its magnitude is just higher than 3%. The magnitude of the effect is different for $K_{\mu3}^0$ (about 6%) and $K_{\mu3}^{\pm}$ (about 4%). But, considering that the $K_{\mu3}$ contribution is by itself small, there is no any change in the overall $\nu_\mu + \overline{\nu}_\mu$ flux. As a consequence, the inclusion of the q^2-dependent $K_{\ell3}$ form factors decreases the $(\nu_\mu + \overline{\nu}_\mu)/(\nu_e + \overline{\nu}_e)$ ratio for the conventional neutrinos by about 3 to 4%, depending on the zenith angle and energy. As one might expect, the effect is small but not completely negligible. Figure 8 illustrates the $K_{\ell3}$ form factor effect for the AN flavor ratio in the presence of a PN contribution. Clearly, it is absent when prompt neutrinos dominate. Thus, we use the lowest PM contribution as predicted in the pQCD model by Thunman et al. [8]. By the evident reasons, there is no effect of any value in the $\nu_e/\overline{\nu}_e$ and $\nu_\mu/\overline{\nu}_\mu$ ratios.

---

[3]At PeV energies, the $\nu_e/\overline{\nu}_e$ ratio becomes a crucial parameter on account of the W resonance in $\overline{\nu}_e e^-$ annihilation.

VI. CONCLUSIONS

The main result of this work consists in the explicit formulas for the semileptonic decay rates (differential and total) of $K^\pm$ and K_L^0 mesons, which take into account the q^2-dependent $K_{\ell 3}$ form factors. The obtained rates differ essentially from those calculated with constant form factors and the total rates are in good agreement with experiment.

With a rather detailed model for nuclear cascade in the atmosphere and with the improved differential $K_{\ell 3}$ rates, we have calculated the ν_e, $\overline{\nu}_e$, ν_μ and $\overline{\nu}_\mu$ spectra at energies 1 to 100 TeV. The calculated spectra are within the limits resulting from the uncertainties in the current data on the primary cosmic ray flux and cross sections for hadron-nucleus interactions at high energies.

The outcome of the inclusion of q^2-dependent $K_{\ell 3}$ form factors into the AN flux calculation is as follows. The electron neutrino flux from K_{e3}^0 and $K_{e3}^\pm$ decays increases by about 3–3.5 %. The $K_{\mu 3}^0$ and $K_{\mu 3}^\pm$ decay contributions into the muon neutrino flux reduces by about 6 and 4 %, respectively, whereas the change in the overall $\nu_\mu + \overline{\nu}_\mu$ flux is completely negligible. If the PN contribution is as slight as predicted by the pQCD model, the change in the neutrino flavor ratio, R, comprises 3 to 4 %. This small systematic effect may only slightly be enhanced by taking account of kaon regeneration or through the variation of the kaon production cross sections within the experimental boundaries. And vise versa, it may be removed, wholly or in part, beyond the multi-TeV energy range if the PN contribution is as large as it follows from the RQPM or QGSM predictions.

The sensitivity of the R to the PN contribution provides a way for an experimental discrimination of this contribution by measuring the relationship between the "muonfull" and "muonless" contained event rates in a neutrino telescope.

ACKNOWLEDGMENTS

[1] E.V.Bugaev, V.A.Naumov, S.I.Sinegovsky, A.Misaki, N.Takahashi and E.S.Zaslavskaya in Proc. the 3rd NESTOR International Workshop, Fortress of Niokastro, Pylos, Greece, 19–21 October, 1993, edited by L. K. Resvanis (Physics Laboratory of the Athens University, Athens) 1994, p. 268.

[2] L.V.Volkova, Yad. Fiz. **31** (1980) 1510

[3] K.Mitsui, Y.Minorikawa and H.Komori, Nuovo Cimento **C9** (1986) 995.

[4] A.V.Butkevich, L.G.Dedenko and I.M.Zheleznykh, Yad. Fiz.**50** (1989) 142.

[5] P.Lipari, Astropart. Phys.**1** (1993) 195.

[6] V.Agrawal, T.K.Gaisser, P.Lipari and T.Stanev, Phys. Rev. **D53** (1996) 1314.

[7] E.V.Bugaev, V.A.Naumov, S.I.Sinegovsky and E.S.Zaslavskaya, Nuovo Cimento **C12** (1989) 41.

[8] M.Thunman, G.Ingelman and P.Gondolo in Proc. of the Workshop on Trends in Astroparticle Physics, Stockholm, Sweden, 22–25 September, 1994, edited by L. Bergström et al. [Nucl. Phys. B (Proc. Suppl.) **43** (1995) 274]; P.Gondolo, G.Ingelman and M.Thunman, Astropart. Phys.**5** (1996) 309.

[9] G.Battistoni, C.Bloise, C.Forti, M.Greco, J.Ranft and A.Tanzini, Astropart. Phys.**4** (1996) 351.

[10] Particle Data Group (R.M.Barnett et al.) Phys. Rev. **D54** (1996) 1.

[11] T.Gaisser, Cosmic Rays and Particle Physics (Cambridge University Press, Cambridge) 1990, p. 89.

[12] V.A.Naumov in Proc. of the International Workshop on ν_μ/ν_e Problem in Atmospheric Neutrinos, Gran Sasso, Italy, 5–6 March, 1993, edited by V.S.Berezinsky and G.Fiorentini (LNGS, L'Aquila, Italy) 1993, p. 25.

[13] L.B.Okun, Leptons and Quarks (Elsevier Science Publishers B.V., North-Holland) 1987, p. 41; J.Bijnens, G.Ecker and J.Gasser in The DAΦNE Physics Handbook, edited by L.Maiani et al. (INFN, Laboratori Nazionali di Frascati) 1992, Vol. I, p. 115.

[14] N.Brene, L.Egardt and B.Qvist, Nucl. Phys. **22** (1961) 553.

[15] V.A.Naumov, T.S.Sinegovskaya and S.I.Sinegovsky in preparation.

[16] A.N.Vall, V.A.Naumov and S.I.Sinegovsky, Yad. Fiz. **44** (1986) 1240 [Sov. J. Nucl. Phys.**44** (1986) 806].

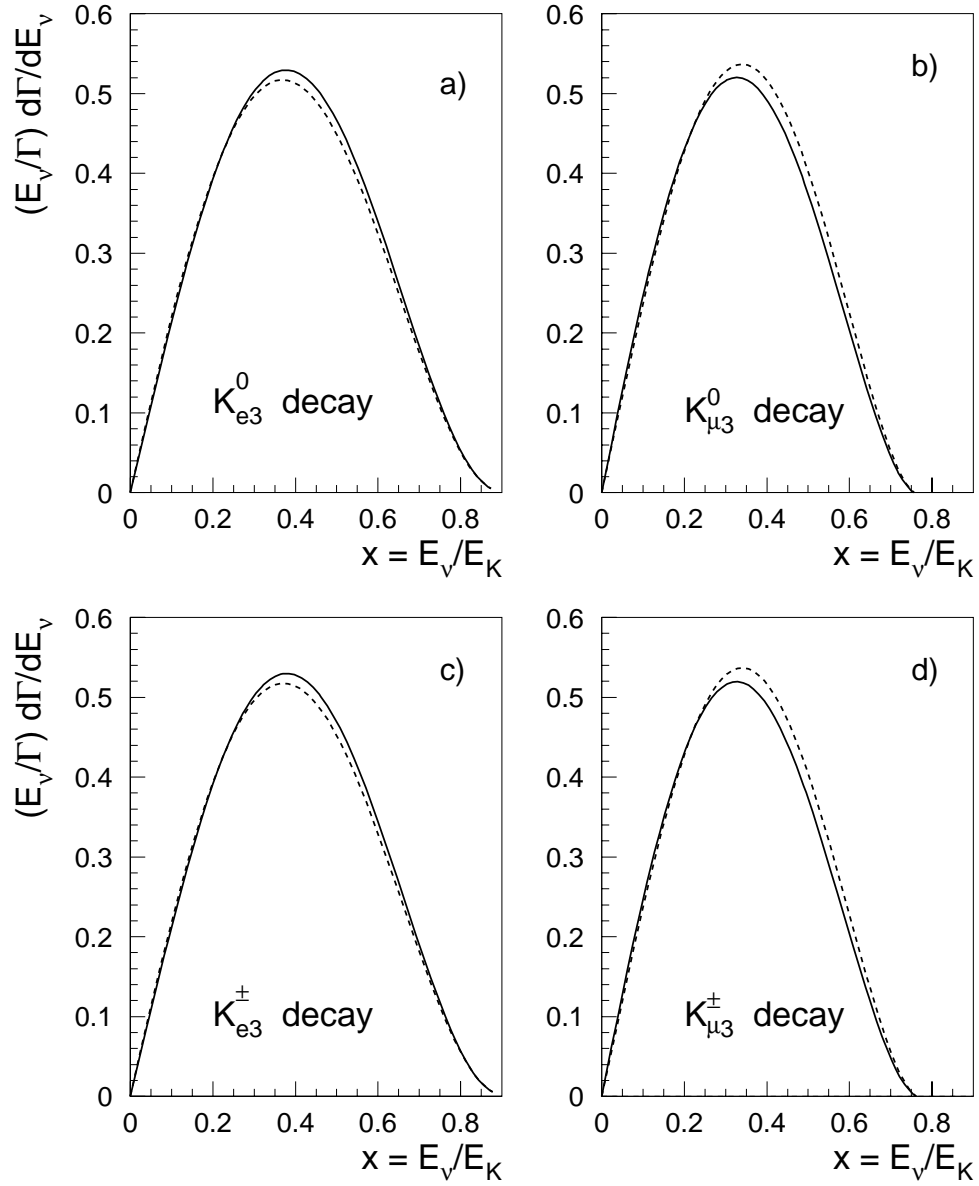[17] S.N.Nikol'sky, I.I.Stamenov and S.Z.Ushev, Zh. Eksp. Teor. Fiz. **87** (1984) 18.

FIG. 1. The normalized x-distributions of (anti)neutrinos in $K_{\ell 3}$ decays, $xF^{\nu}_{K_{\ell 3}}(x)$, calculated with $f_+ = f_+(0)$ (dashed curves) and with q^2-dependent f_+ (solid curves).
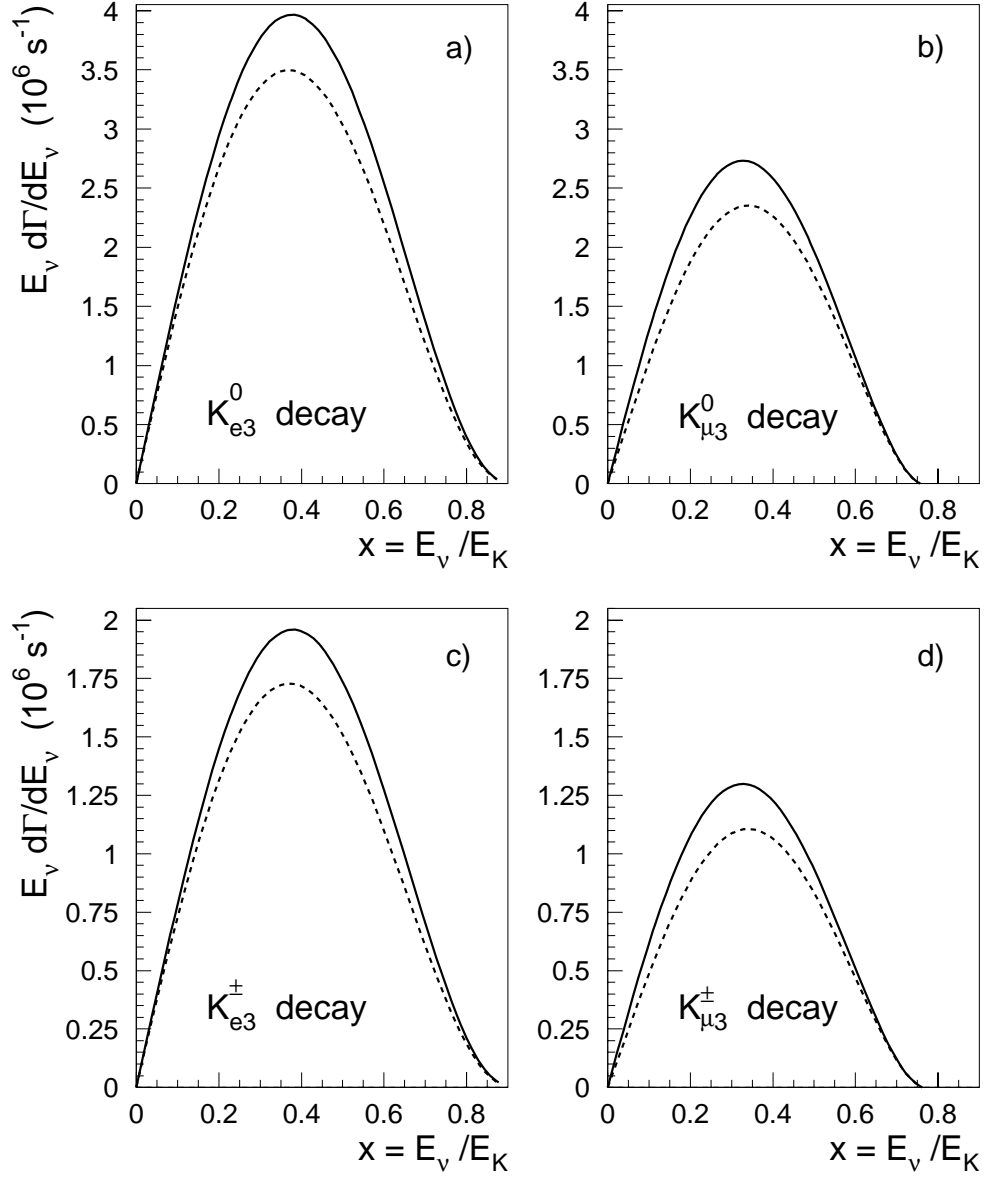
FIG. 2. The absolute x-distributions of (anti)neutrinos in $K_{\ell 3}$ decays, $E_\nu d\Gamma^\nu_{K_{\ell k}}/dE_\nu$, calculated with $f_+ = f_+(0)$ (dashed curves) and with q^2-dependent f_+ (solid curves).
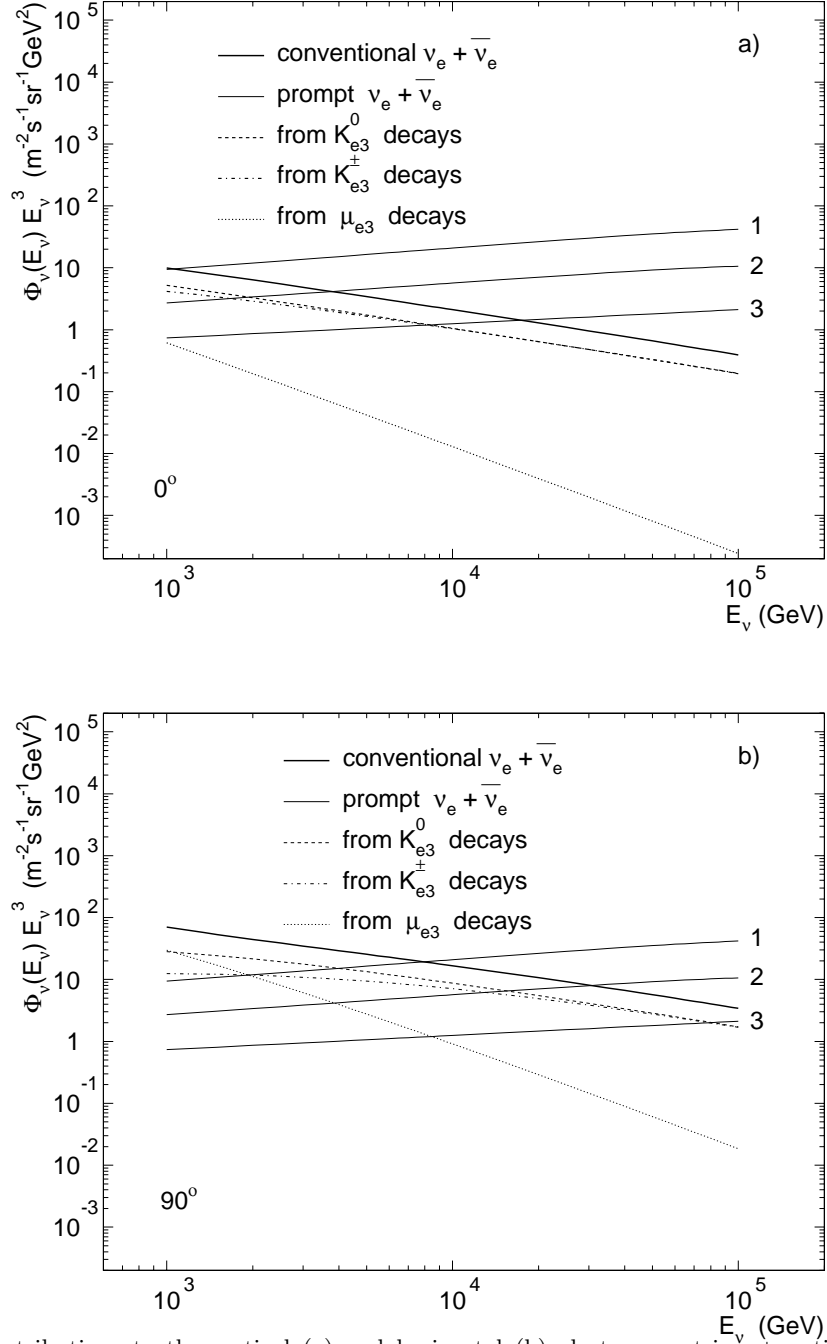
FIG. 3. Different contributions to the vertical (a) and horizontal (b) electron neutrino + antineutrino fluxes. The PN contributions calculated in RQPM, QGSM and pQCD are marked "1", "2" and "3", respectively.
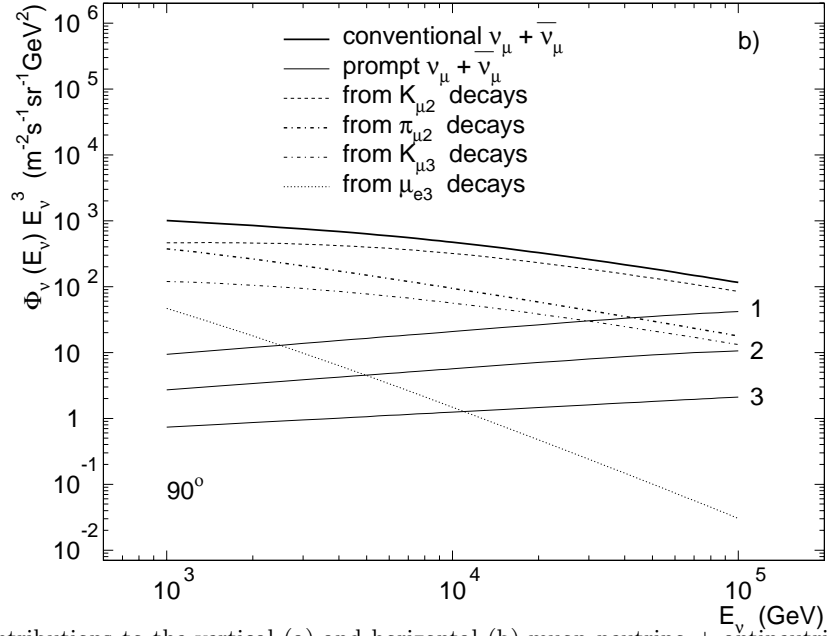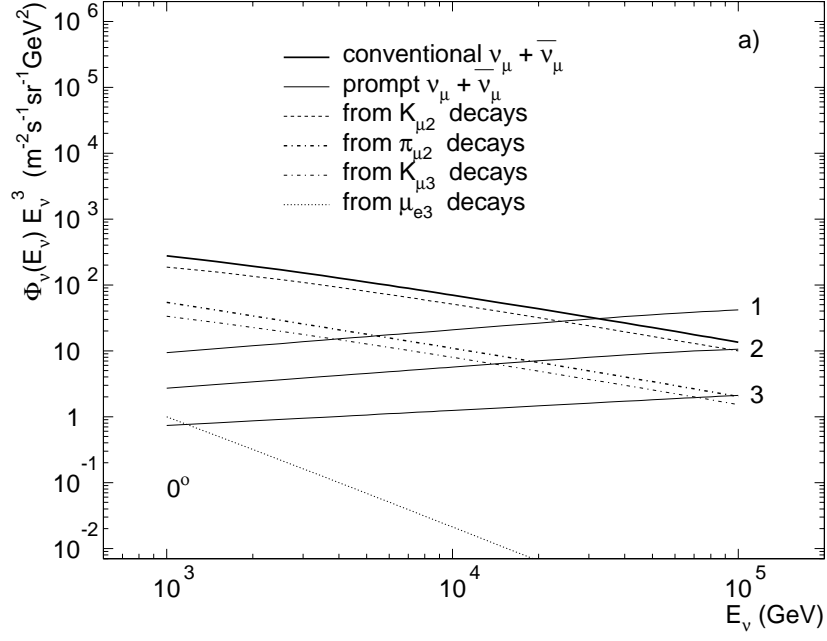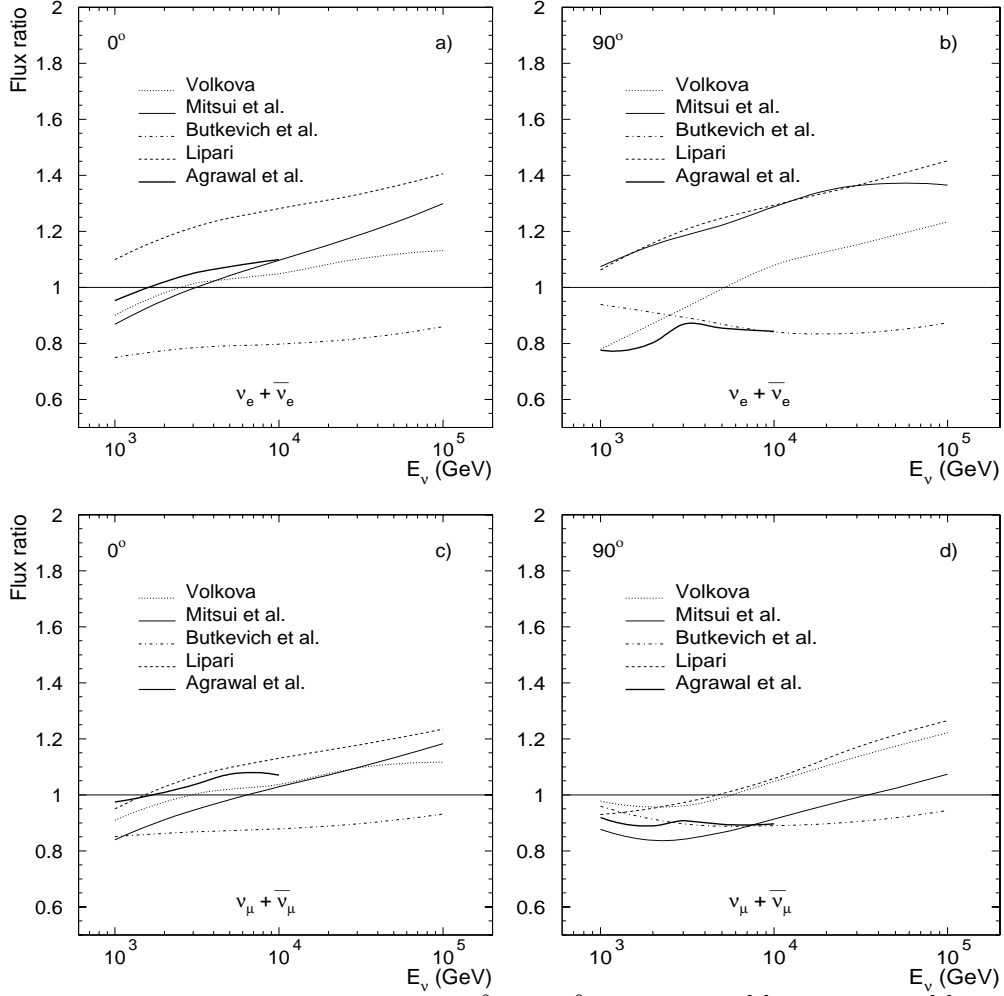
FIG. 4. Different contributions to the vertical (a) and horizontal (b) muon neutrino + antineutrino fluxes. The PN contributions calculated in RQPM, QGSM and pQCD are marked "1", "2" and "3", respectively.

FIG. 5. Conventional $\nu_e + \overline{\nu}_e$ and $\nu_\mu + \overline{\nu}_\mu$ fluxes at $\vartheta = 0°$ and $90°$ from Volkova [2], Mitsui et al. [3], Butkevich et al. [4], Lipari [5] and Agrawal et al. [6], normalized to the fluxes calculated in this work.
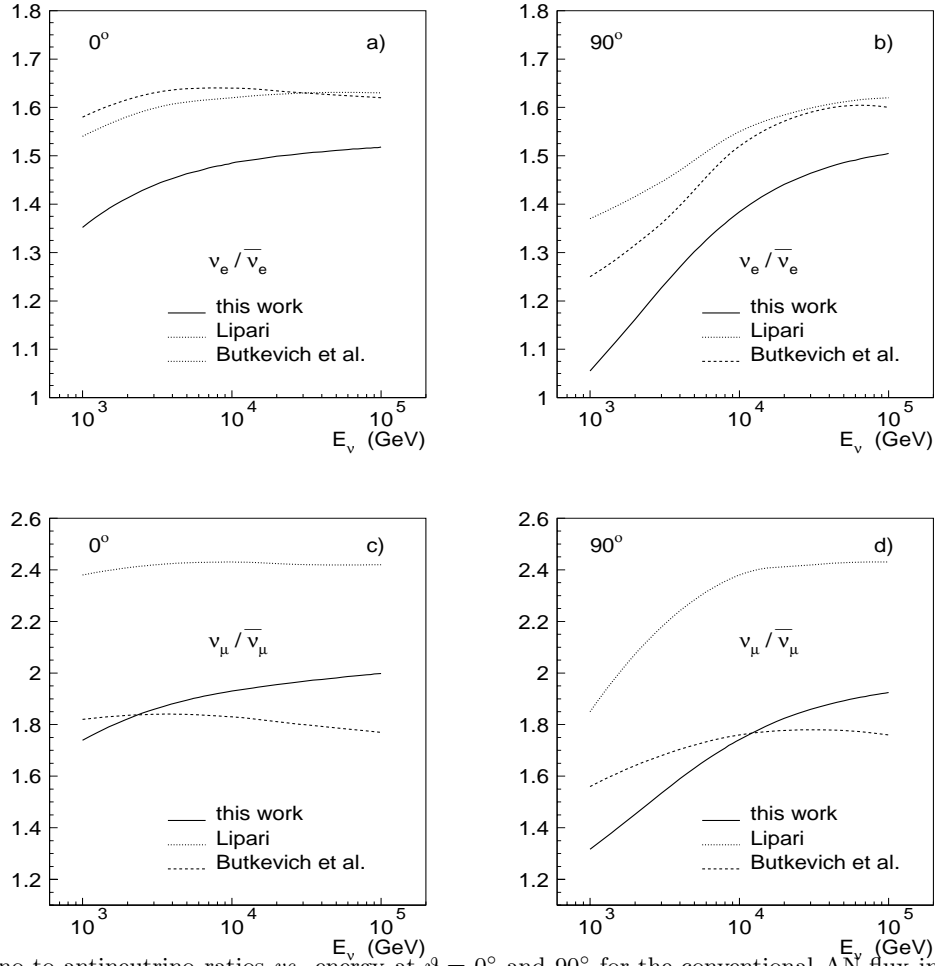
FIG. 6. Neutrino to antineutrino ratios *vs.* energy at $\vartheta = 0°$ and $90°$ for the conventional AN flux in comparison with the results by Lipari [5] and Butkevich et al. [4].
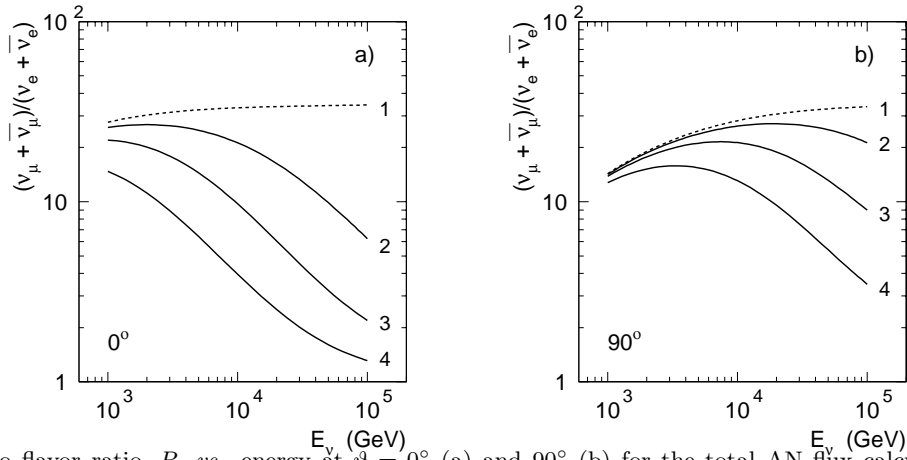

FIG. 7. Neutrino flavor ratio, R, *vs.* energy at $\vartheta = 0°$ (a) and $90°$ (b) for the total AN flux calculated without the PN contribution (1) and with taking it into account using the three models for charm production, pQCD (2), QGSM (3) and RQPM (4).
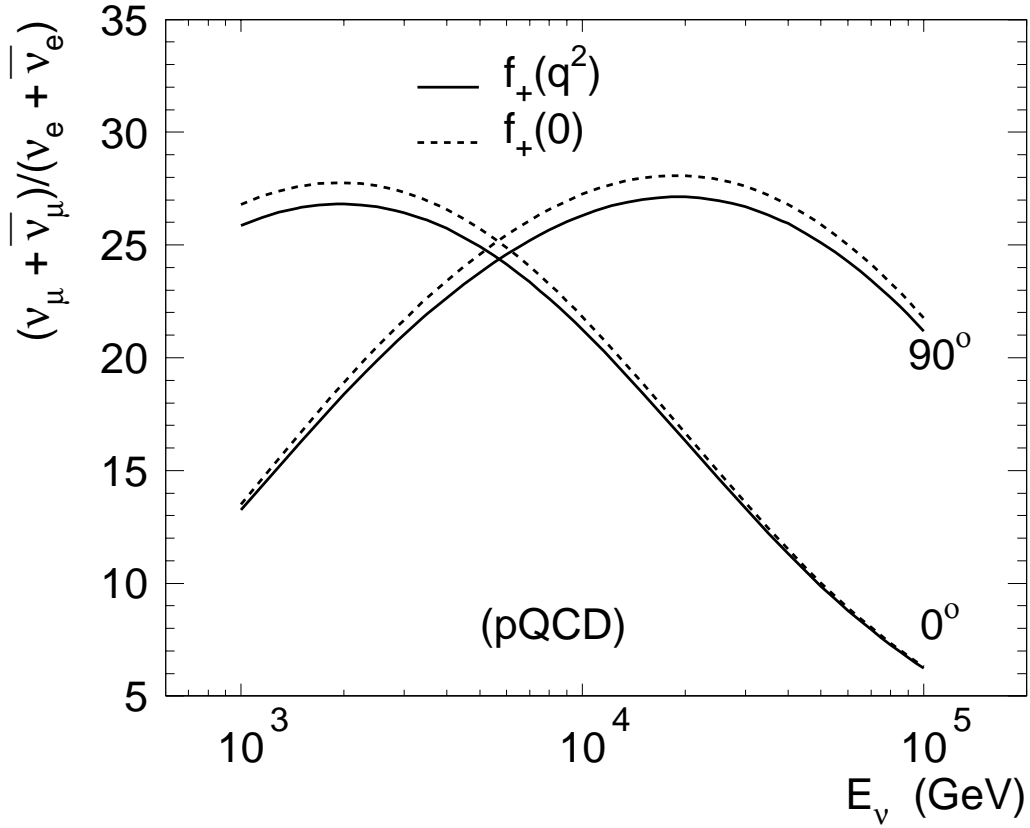
FIG. 8. Effect of the q^2-dependent $K_{\ell 3}$ form factors for the neutrino flavor ratio at $\vartheta = 0°$ and $90°$. The PN contribution is taking into account using the pQCD model by Thunman et al. [8]. The dashed and solid curves are for the constant and q^2-dependent form factors, respectively.